

Giant Goos-Hänchen Shift in Graphene Double-barrier Structures

Yu Song,^{1,*} Han-Chun Wu,² and Yong Guo¹

¹*Department of Physics and State Key Laboratory of Low-Dimensional Quantum Physics, Tsinghua University, Beijing 100084, People's Republic of China*

²*CRANN and School of Physics, Trinity College Dublin, Dublin 2, Ireland*

(Dated: August 6, 2018)

We report giant Goos-Hänchen shifts [F. Goos and H. Hänchen, *Ann. Phys.* **436**, 333 (1947)] for electron beams tunneling through graphene double barrier structures. We find that inside the transmission gap for the single barrier, the shift displays sharp peaks with magnitudes up to the order of electron beam width and rather small full-widths-at-half-maximum, which may be utilized to design valley and spin beam splitters with wide tunability and high energy resolution. We attribute the giant shifts to quasibound states in the structures. Moreover, an induced energy gap in the dispersion can increase the tunability and resolution of the splitters.

In optics, it is well-known that a light beam undergoes a lateral shift when it is totally reflected from a dielectric interface.¹ This phenomena is referred to as the Goos-Hänchen (GH) shift² and can be theoretically explained based on the reshaping of the wave packet.³ Analogies of the GH shift have been widely considered in various fields, including acoustics,⁴ electronics,⁵⁻⁷ relativistic corrections,⁸ atomic optics,⁹ and neutronics.¹⁰

Recently, the analogy for the massless electron has become of interest¹¹⁻¹⁶ since discovery of graphene, a monolayer of sp^2 bonded carbon atoms.¹⁷ It has been reported that the GH shift plays an important role in the group velocity of quasiparticles along interfaces of graphene p - n junctions,^{11,12} whereby a twofold degeneracy on top of the usual spin and valley degeneracies can be introduced¹¹ and coherent buffers and memories can be realized in graphene p - n - p waveguides.¹² The valley-dependent GH shift^{15,16} based on strained graphene has been very recently utilized by Zhai *et al.* to design a valley beam splitter.¹⁶ We note that, to effectively realize the proposed splitter, the difference of GH shifts for valley K and K' should be larger than the longitudinal width of the electron beam defined as $w_y = w_b \cos^{-1} \bar{\alpha}$, where w_b and $\bar{\alpha}$ are the waist width and incident angle of the electron beam, respectively. This condition also ensures the validity of the stationary-phase approximation,¹⁸ which is widely used in GH shift calculation¹¹⁻¹⁶ especially for resonant transmission.¹⁹ Considering a typical beam divergence ($\delta\bar{\alpha} \equiv \lambda_F/\pi w_b$ with λ_F the Fermi wave-length) of 1° - 0.1° ,¹⁹ w_b is $180\lambda_F$ - $1800\lambda_F$. In a n - p - n single barrier structure (SBS),¹⁶ this condition may not be met without properly selecting the structural parameters. On the other hand, the spin-dependent GH shift was also proposed to spatially split spin beams, based on a SBS formed by a local magnetic field²⁰ and an electrostatic potential in a two-dimensional electron gas (2DEG).⁷ However, the displacements of the spin-dependent GH shifts are also found to be insufficient.⁷ Therefore, finding a suitable structure to effectively implement these ideas is one of the main issues in such an exciting field.

In this letter, we report a giant GH shift of elec-

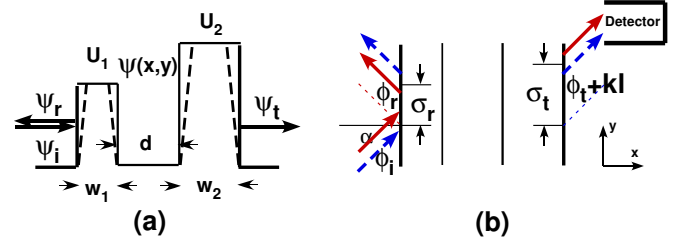


FIG. 1. (color online) (a) Sectional and (b) top schematic diagrams for a particle quantum tunneling through a graphene DBS, with the two barriers of width $w_{1(2)}$, height $U_{1(2)}$, and distance d between them. $l = w_1 + w_2 + d$ is the total width of the structure. In (a), the dashed lines show smooth electric potentials with distributions of error functions and transition regions' widths of $0.1w_{1(2)}$. In (b), the upper (red solid) and lower (blue dashed) components have their locus at $\pm\delta/2$, $\sigma_r \mp \delta/2$, and $\sigma_t \pm \delta/2$ for the incident, reflected and transmitted beams, respectively. A detector placed in a proper position of the outgoing region can detect the giant GH shift.

tron beams tunneling through a double barrier structure (DBS) in graphene. We find that inside the transmission gap (TG) for the constituted single barrier²¹ the GH shift displays sharp peaks which are absent in the SBS cases and were attributed to the quasibound states formed in the DBS. Remarkably, we find that the magnitudes of the peaks are much larger than the maximum magnitude in the corresponding SBS and can easily achieve the order of w_y . Together with the rather small full-widths at half-maximum (FWHM) of the peaks, this giant GH shift can be used for designing valley and spin beam splitters with wide tunability and high energy resolution. We also investigate the effects of the structural asymmetry of the DBS and the induced energy gap in the linear dispersion. The results show that the former suppresses the GH shift while the latter enhances it, which increases the controllability of devices based on the GH shift.

To investigate the GH shift in graphene DBSs, we consider an incident beam well collimated around some transverse wave vector $\bar{q} \in (-q_m, q_m)$ ($q_m = E/\hbar v_F$) [corresponding to $\bar{\alpha} = \arcsin(\bar{q}/q_m)$], quantum tunneling through a graphene DBS as sketched in Fig. 1. The

Dirac equation can be written as:

$$(v_F \boldsymbol{\sigma} \cdot \mathbf{p} + \Delta \sigma_z + U) \Psi = E \Psi, \quad (1)$$

where $v_F \approx 10^6 m/s$ is the Fermi velocity, $\boldsymbol{\sigma} = (\sigma_x, \sigma_y)$ is the pseudospin operator given by Pauli's matrices, $\mathbf{p} = (p_x, p_y)^T$ is the momentum operator, $\Delta = mv_F^2(\Delta_{SO})$ is the energy gap owing to the sublattice symmetry breaking²² (the spin-orbit interaction²³), and $U = U_{1(2)}$ in the barriers while $U = 0$ elsewhere. The wave packets of the incident and associated reflected and transmitted beams at the two terminals of the DBS can be given by

$$\Psi^i(x, y) = \frac{1}{\sqrt{2}} \int_{-q_m}^{q_m} dq f(q - \bar{q}) e^{ik(q)x + iqy} \begin{pmatrix} e^{-i\alpha'(q)/2} \\ \lambda e^{i\alpha'(q)/2} \end{pmatrix}, \quad (2a)$$

$$\Psi^r = \frac{1}{\sqrt{2}} \int_{-q_m}^{q_m} dq r(q) f(q - \bar{q}) e^{-ik(q)x + iqy} \begin{pmatrix} -ie^{i\alpha'(q)/2} \\ \lambda ie^{-i\alpha'(q)/2} \end{pmatrix}, \quad (2b)$$

$$\Psi^t = \frac{1}{\sqrt{2}} \int_{-q_m}^{q_m} dq t(q) f(q - \bar{q}) e^{ik(q)x + iqy} \begin{pmatrix} e^{-i\alpha'(q)/2} \\ \lambda e^{i\alpha'(q)/2} \end{pmatrix}. \quad (2c)$$

Here each plane wave of the spinor form is a solution of Eq. (1), and a basis is used to ensure that the product of the upper and lower components is real.¹¹ $f(q - \bar{q})$ is the angular spectral distribution which can be assumed to be of Gaussian profile, $w_y e^{-w_y^2(q - \bar{q})^2/2}$. $k(q) = \sqrt{q_m^2 - (\Delta/\hbar v_F)^2 - q^2}$ is the longitudinal wave vector and $\alpha'(q) = \sin^{-1}(\hbar v_F q / \sqrt{E^2 - \Delta^2})$ is the phase angle. Due to the induced energy gap Δ , α' is usually different from the incident angle and a factor $\lambda = \sqrt{E^2 - \Delta^2}/(E + \Delta)$ appears in the lower component of the spinors. For the reflected and transmitted beams, $r(q) = |r(q)|e^{i\phi_r(q)}$ and $t(q) = |t(q)|e^{i\phi_t(q)}$ are the reflection and transmission coefficients respectively, which can be determined by the continuities of each component and calculated by the standard transfer-matrix method.²⁴

From the stationary-phase approximation,¹⁸ the vanishing of the gradient of the total phase in direction gives the locus of the steady wave packet peak. Due to the spinor nature of graphene, the loci of the two components in a beam are found to be different.¹¹ For the incident and transmitted beam, the upper component exceeds the lower one with a distance of δ ($\delta = 1/k$), while for the reflected beam the inverse becomes the case [see, Fig.1(b)]. The deviation between the loci of the reflected (transmitted) and the incident beams thus gives corresponding GH shift, $\sigma_r^\pm = -d\phi_r/dq|_{\bar{q}} \mp \delta$ and $\sigma_t^\pm = -d\phi_t/dq|_{\bar{q}}$, where $\bar{\phi}_t \equiv \phi_t + kl$. Note the GH shift in reflection is component dependent while the shift in transmission is not [see, Fig.1(b)]. We'd like to use $\sigma_r = -(d\phi_r/dq)|_{\bar{q}}$ to describe the average shift in reflection.

Fig. 2(a) shows the calculated GH shift for a symmetric graphene DBS as a function of E at a fixed $\bar{\alpha} = 10^\circ$. In this calculation, $\Delta = 0$. To make sure the electron density of states coincides with a true system and the

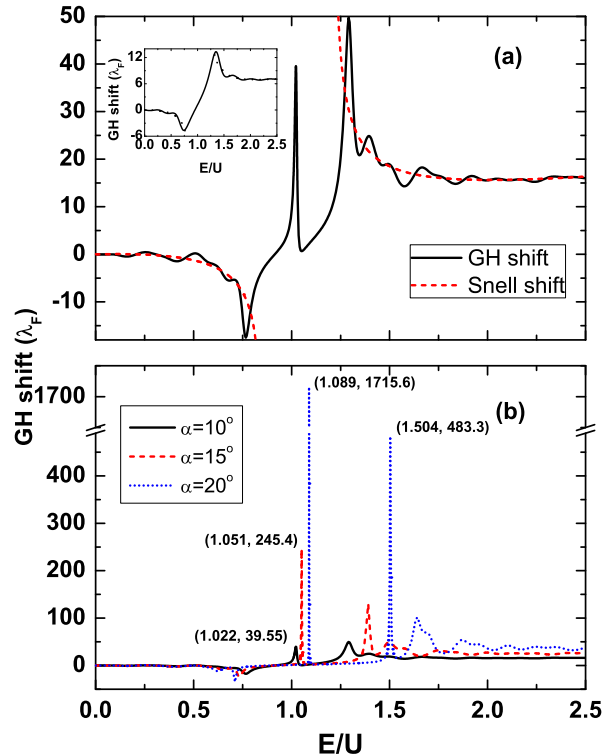


FIG. 2. (color online) (a) The GH shift (solid) in a symmetric graphene DBS [$U = U_1 = U_2 = 62$ meV, $w_1 = w_2 = 100$ nm, $d = 50$ nm] as a function of the incident energy at $\bar{\alpha} = 10^\circ$. The insert shows the GH shift in a SBS with the same barrier height and width. The dashed line indicate the semi-classical shift predicted by the Snell's law, which has no definition in the TG. (b) The dependence of the shift sharp peak(s) on the incident angle, $\bar{\alpha} = 10^\circ, 15^\circ$, and 20° . The positions and heights of the four giant GH shift peaks are marked.

system stays in a ballistic regime, typical values are used: $U = 62$ meV, $w = 100$ nm, and $d = 50$ nm. These parameters also ensure the legitimacy of the stationary-phase approximation.^{18,19,25} One can see from Fig. 2(a) that outside the TG, the GH shift shows the same trend as the shift predicted by geometric optics using Snell's law.^{13,16} Moreover, the GH shift oscillates around the Snell shift as it is enhanced (suppressed) at $k_i w_i = N\pi$ [$k_i w_i = (N - 1/2)\pi$] with $N = 1, 2, 3, \dots$ where resonant (antiresonant) tunneling happens. Note, the positive peak nearest the TG (denoting as P_{SBS}) which has the maximum magnitude for tunneling through a SBS cannot be enhanced to the order of the longitude beam width without properly selecting the structural parameters.

Remarkably, a significantly sharp peak with a magnitude comparable to P_{SBS} appears inside the TG [around

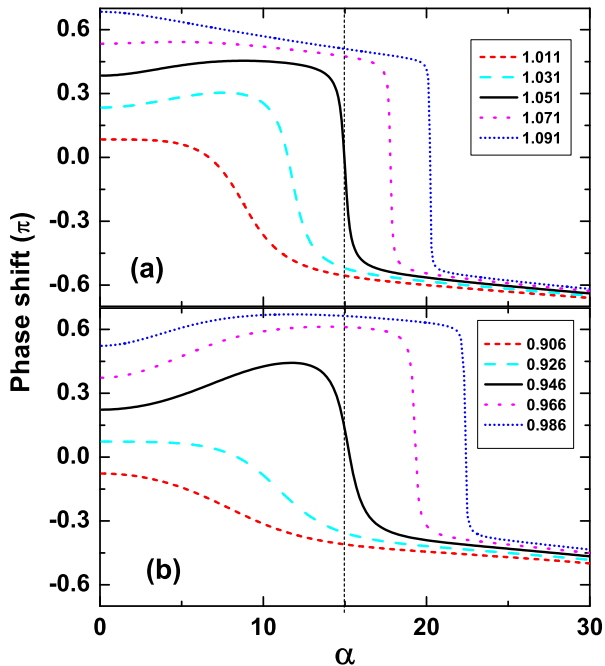


FIG. 3. (color online) The phase shift of the transmitted beam vs. the incident angle for beams with different E/U shown in the figure. (a)/(b) for a rectangular/smooth DBS.

$E/U = 1$ in Fig. 2(a)]. This is absent in the case of electron beams tunneling through graphene SBSs [see the inset of Fig. 2(a)]. One can clearly see from Fig. 2(b) that with increasing incident angle the peak value of the GH shift dramatically increases. At $\bar{\alpha} = 20^\circ$, the peak value reaches $\sim 1700\lambda_F$ (~ 16000 nm) which is about ten times of the corresponding P_{SBS} and is in the order of the longitudinal beam width. Therefore, the obtained results suggest that the valley splitter based on this structure can be realized with much looser conditions, since giant GH shift for valley $K(K')$ can be obtained inside the TG while the GH shift for valley $K'(K)$ retains the order of λ_F . In addition, due to the rather small FWHM the splitter will possess a much higher energy or wave vector resolution.

It is surprising that the GH shift in a graphene DBS possesses such giant magnitudes, since the shift along a single interface or through a SBS (inside the TG) is of the order of Fermi wave-length λ_F .^{11–16} Here, we attribute it to the quasibound states in the DBS, which are formed by the evanescent waves in the two barriers. It is well-known that plane waves with different q generally present different phase shifts, leading to the reshaping of the wave packet and thus the GH shift of the electron

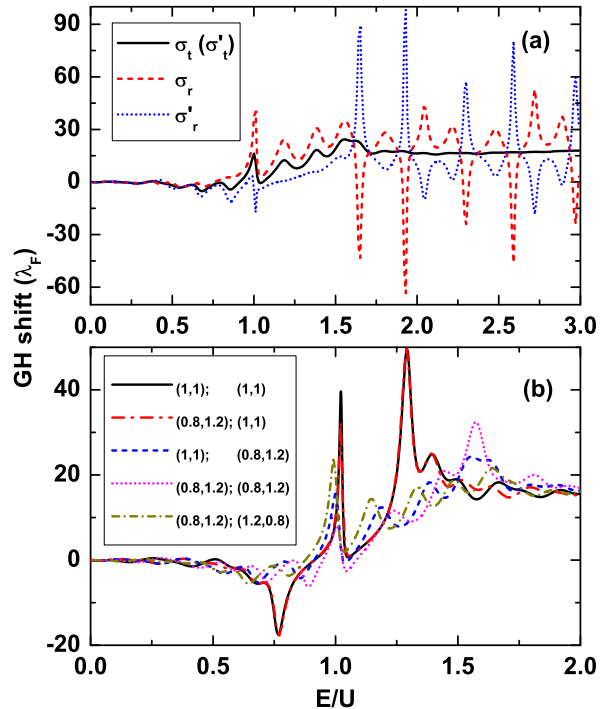


FIG. 4. (color online) (a) GH shifts in transmission and reflection for an asymmetric DBS with $U = 62$ meV, $U_1 = 0.8U$, $U_2 = 1.2U$, $w_1 = w_2 = w = 100$ nm, and $d = 50$ nm. (b) GH shifts in transmission for different cases of structural asymmetries with the parameters $(w_1/w, w_2/w)$ and $(U_1/U, U_2/U)$ in the sequence given in the figure. For all cases, $\bar{\alpha} = 10^\circ$.

beam. In our case, when the center plane wave is aligned to the quasibound state, multiple interferences will arise through the quasistanding waves between the two barriers. This will lead to a remarkable difference in the phase shifts between the center plane wave and adjacent ones [see Fig. 3(a)]. Accordingly, a giant GH shift for such an electron beam is present inside the TG. One can also see clearly from Fig. 3(a) that with the increasing E/U of the beam, the incident angle which shows the biggest slope of $-\partial\phi_r/\partial\alpha$ also increases, which is consistent with Fig. 2(b). Thus, the observed giant GH shift inside the TG is due to the quasibound states formed in graphene DBSs.

One may wonder how the smoothness of realistic barriers will affect the magnitude of the GH shift. To answer this problem, we consider a realistic potential which varies smoothly on the scale of the graphene lattice constant and adopt a typical potential profile¹⁶ of $U(x) = 0.5U[\text{erf}(2x/L_b - 2) + \text{erf}(2(w-x)/L_b - 2)]$, where $\text{erf}(x)$ is the error function and the width of the transition region is set as $L_b = 0.1w$ (see Fig. 1(a)). We calculated the transmission coefficient, phase shift, and also

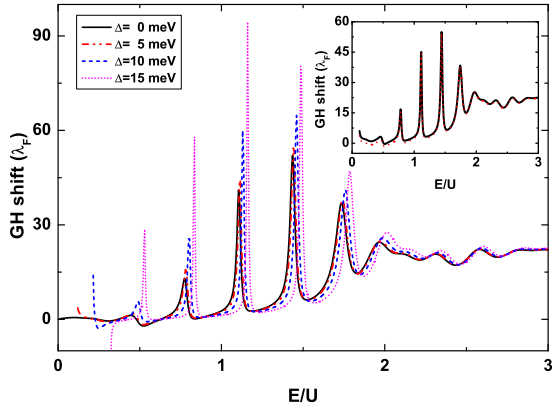


FIG. 5. (color online) The GH shift in transmission through a graphene DBS with $w_1 = w_2 = 50$ nm, $d = 100$ nm and $U = U_1 = U_2 = 50$ meV. The induced gap is $\Delta = 0, 5, 10, 15$ meV as indicated in the figure. Inset: the GH shifts for the reflected and transmitted beams for $\Delta = 5$ meV in the same structure. For all cases, $\bar{\alpha} = 20^\circ$.

the GH shift. Similar results have been achieved. Fig. 3(b) shows the phase shifts as a function of incident angle for a smooth DBS. Compared with the case of a rectangular DBS with the same $\bar{\alpha} = 15^\circ$, the giant GH shift for a smooth DBS appears at a lower incident energy (from $E/U = 1.051$ to 0.946) and the magnitude of the giant GH peaks decreases from $245.4\lambda_F$ to $67.4\lambda_F$. To achieve the GH shift in the order of the longitude beam width, one can increase the incident angle (about 23°). Thus the smoothness of the potential barriers will not restrict the use of the giant GH shift. For convenience, we will adopt the rectangular model in the following discussions.

We now study the effect of the structural asymmetry of the DBS which may be introduced during sample preparation and gate control, i.e., the two barriers have different widths and/or heights. Fig. 4 shows the GH shifts in transmission and reflection for asymmetric DBSs. Interestingly, one can see from Fig. 4(a) that the GH shift in reflection crucially depends on which terminal the beam is being reflected from, where σ_r and σ_t (σ'_r and σ'_t) mean the GH shift in reflection and transmission for electron beams incident on the U_1 (U_2) terminal (as shown in Fig. 1). We would like to point out that σ_r and σ'_r are found to follow the relation of $\sigma_r + \sigma'_r = 2\sigma_t$ which holds for any asymmetric DBSs and can be understood by the relation between the reflection and transmission coefficients. Through the scattering matrix,²⁴ we can get $t' = t$ and $r' = -tr^*/t^*$, which imply $\bar{\phi}'_t = \bar{\phi}_t$ and $\phi_r + \phi'_r = 2\bar{\phi}_t$, respectively. r (r') and t (t') are the reflection and transmission coefficients of the beam reflected from or tunneling through the U_1 (U_2) terminal, where the term kl has been contained in t and t' . Using the definition of GH shift, we get $\sigma_t = \sigma'_t$ and $\sigma_r + \sigma'_r = 2\sigma_t$. Note for a symmetrical DBS, $\bar{\phi}_t = \phi_r$ ($\bar{\phi}'_t = \phi'_r$) thus $\phi'_r = \phi_r$, which

indicates that the two GH shifts in reflection will become identical in this case.

We now take σ_t (σ'_t) as a target to evaluate the effect due to the structural asymmetries. As shown in Fig. 4(b), the effect of structural asymmetry always suppresses the GH shift inside the TG. For the case of barriers with the same height but different widths, the structural asymmetry only decreases the magnitude of the GH shift inside the TG while not moving the peak position. For the case of barriers of different heights, the effect of structural asymmetry not only decreases the magnitude of the GH shift inside the TG but also makes the peak position shift. Moreover, the FWHM of the peak of the GH shift increases.

Fig. 5 shows the GH shift for the transmitted beam in a graphene DBS with different induced energy gaps in the linear dispersion. As is seen, when there is a nonzero gap, the GH shift has no definition for $E^2 \cos^2 \bar{\alpha} < \Delta^2$ as the electron cannot propagate freely even in the non-modulated regions. Meanwhile, the GH shifts for the reflected and transmitted beams differ (see insert in Fig. 5). With increasing induced energy gap, the peak positions of the GH shift inside the TG move to higher energies. Moreover, the magnitudes of the peaks increase and the FWHMs become even smaller, which increases the tunability and energy resolution of the valley or spin splitter device. The underlying physics is that, the presence of energy gap increases the modulus of the longitudinal wave vector (κ), which makes a stronger multiple interference effect and thus a bigger GH shift at a little higher energy.

In summary, we have theoretically calculated the GH shifts of reflected and transmitted electron beams in a graphene DBS. Interestingly, we found that the GH shift displays sharp peaks inside the TG for the constituted SB, which are absent in the graphene SBS cases and can be attributed to the quasibound states formed in the DBS. The reported giant GH shift can be detected in the transmitted beam by placing a detector in the outgoing region and far away from the incident position (see Fig. 1(b)). In the TG, the detector will collect no electrons unless the incident energy is aligned to the quasibound states. The results obtained in this work suggest the feasibility of making valley splitter based on graphene DBSs. The tunability and energy resolution of the splitter can be further increased by an induced energy gap in the linear dispersion. By the spin-dependent giant GH shift, a spin beam splitter restricted by the small magnitude of the GH shift⁷ may be realized in 2DEG or graphene based DBSs now.

This work was supported by the NSFC (10974109 and 11174168), the SRFDP (20100002110079), and the 973 Program (2011CB606405). HCW was grateful to the SFI Short Term Travel fellowship support during his stay at PKU and thanks Dr. Cormac Ó Coileáin for reading the paper and giving valuable comments.

-
- * kwungyusung@gmail.com
- ¹ H. K. V. Lotsch, *Optik (Stuttgart)* **32**, 116 (1970); *ibid.* **32**, 189 (1970); *ibid.* **32**, 299 (1971); *ibid.* **32**, 553 (1971).
 - ² F. Goos and H. Hänchen, *Ann. Phys.-Berlin* **436**, 333 (1947); *ibid.* **440**, 251 (1949).
 - ³ K. V. Artmann, *Ann. Phys.* **437**, 87 (1948).
 - ⁴ R. Briers, O. Leroy, and G. Shkerdinb, *J. Acoust. Soc. Am.* **108**, 1624 (2000).
 - ⁵ R.-H. Renard, *J. Opt. Soc. Am.* **54**, 1190 (1964); J. L. Carter and H. Hora, *ibid.* **61**, 1640 (1971).
 - ⁶ S. C. Miller, Jr. and N. Ashby, *Phys. Rev. Lett.* **29**, 740 (1972).
 - ⁷ L. Yuan *et al.* *Eur. Phys. J. B* **85**, 8 (2012); X. Chen, X.-J. Lu, Y. Wang, and C.-F. Li, *Phys. Rev. B* **83**, 195409 (2011); X. Chen, C.-F. Li, and Y. Ban, *ibid.* **77**, 073307 (2008).
 - ⁸ D. M. Fradkin and R. J. Kashuba, *Phys. Rev. D* **9**, 2775 (1974); *ibid.* **10**, 1137 (1974).
 - ⁹ J.-H. Huang, Z.-L. Duan, H.-Y. Ling, and W.-P. Zhang, *Phys. Rev. A* **77**, 063608 (2008).
 - ¹⁰ Victor-O. de Haan, J. Plomp, T. M. Rekveldt, W. H. Kraan, A. A. van Well, R. M. Dalgliesh, and S. Langridge, *Phys. Rev. Lett.* **104**, 010401 (2010).
 - ¹¹ C. W. J. Beenakker, R. A. Sepkhanov, A. R. Akhmerov, and J. Tworzydło, *Phys. Rev. Lett.* **102**, 146804 (2009).
 - ¹² L. Zhao and S. F. Yelin, *Phys. Rev. B* **81**, 115441 (2010).
 - ¹³ X. Chen, J.-W. Tao, and Y. Ban, *Eur. Phys. J. B* **79**, 203 (2011).
 - ¹⁴ M. Sharma and S. Ghosh, *J. Phys.: Condens. Matter* **23**, 055501 (2011); P. M. Krstaji and P. Vasilopoulos, *ibid.* **23**, 135302 (2011).
 - ¹⁵ Z. Wu, F. Zhai, F. M. Peeters, H. Q. Xu, and K. Chang, *Phys. Rev. Lett.* **106**, 176802 (2011);
 - ¹⁶ F. Zhai, Y. Ma, and K. Chang, *New J. Phys.* **13**, 083029 (2011).
 - ¹⁷ K. S. Novoselov, A. K. Geim, S. V. Morozov, D. Jiang, M. I. Katsnelson, I. V. Grigorieva, S. V. Dubonos, and A. A. Firsov, *Nature (London)* **438**, 197 (2005); Y. Zhang, Y. W. Tan, H. L. Stormer, and P. Kim, *Nature (London)* **438**, 201 (2005).
 - ¹⁸ C.-F. Li, *Phys. Rev. Lett.* **91**, 133903 (2003).
 - ¹⁹ C.-F. Li and Q. Wang, *Phys. Rev. E* **69**, 055601(R) (2004).
 - ²⁰ F. Zhai and H. Q. Xu, *Phys. Rev. Lett.* **94**, 246601 (2005).
 - ²¹ The transmission gap is a region where the longitudinal wave vector under a single barrier becomes imaginary. See, for example, X. Chen and J.-W. Tao, *Appl. Phys. Lett.* **94**, 262102 (2009).
 - ²² S. Y. Zhou, G. H. Gweon, A. V. Federov, P. N. First, W.A. de Heer, D. H. Lee, F. Guinea, A. H. Castro Neto, and A. Lanzara, *Nat. Mater.* **6**, 770 (2007).
 - ²³ C. L. Kane and E. J. Mele, *Phys. Rev. Lett.* **95**, 226801 (2005).
 - ²⁴ M. Born and E. Wolf, *Principles of optics: electromagnetic theory of propagation, interference and diffraction of light* Oxford, Pergamon Press, 1964.
 - ²⁵ A. M. Steinberg and R. Y. Chiao, *Phys. Rev. A* **49**, 3283 (1994).